HHS Public Access

Author manuscript

Cell Rep. Author manuscript; available in PMC 2017 August 02.

Published in final edited form as:

Cell Rep. 2017 June 27; 19(13): 2645–2656. doi:10.1016/j.celrep.2017.06.013.

A critical analysis of the role of SNARE protein SEC22B in antigen cross-presentation

S Julia Wu[1,2], **Yashar S Niknafs**[2,3], **Stephanie H Kim**[1,2], **Katherine Oravecz-Wilson**[4], **Cynthia Zajac**[4], **Tomomi Toubai**[4], **Yaping Sun**[4], **Jayendra Prasad**[4], **Daniel Peltier**[5], **Hideaki Fujiwara**[4], **Israel Hedig**[4], **Nathan Mathewson**[6], **Rami Khoriaty**[4], **David Ginsburg**[4,7,8,9], and **Pavan Reddy**[1,4,10]

[1]Program in Immunology, University of Michigan Medical School, Ann Arbor, MI 48109, USA

[2]Medical Scientist Training Program, University of Michigan Medical School, Ann Arbor, MI 48109, USA

[3]Cellular & Molecular Biology Program, University of Michigan Medical School, Ann Arbor, MI 48109, USA

[4]Department of Internal Medicine, Division of Hematology/Oncology, Michigan Medicine, Ann Arbor, MI 48109, USA

[5]Department of Pediatrics & Communicable Diseases, Division of Pediatric Hematology/Oncology, Michigan Medicine, Ann Arbor, MI 48109, USA

[6]Dana Farber Cancer Institute, Harvard University, Cambridge, MA 02215, USA

[7]Department of Human Genetics, University of Michigan Medical School, Ann Arbor, MI 48109, USA

[8]Howard Hughes Medical Institute, University of Michigan, Ann Arbor, MI 48109, USA

[9]Life Sciences Institute, University of Michigan, Ann Arbor, MI 48109, USA

Abstract

Cross-presentation initiates immune responses against tumors and viral infections by presenting extracellular antigen on MHC I to activate $CD8^+$ T cell-mediated cytotoxicity. *In vitro* studies in dendritic cells (DCs) established SNARE protein SEC22B as a specific regulator of cross-presentation. However, the *in vivo* contribution of SEC22B to cross-presentation has not been tested. To address this, we generated DC-specific *Sec22b* knockout (*CD11c-Cre Sec22b*$^{fl/fl}$) mice.

[10]Lead contact, reddypr@med.umich.edu.

Competing interests

For all authors, there are no competing interests to disclose.

Author Contributions

Conceptualization, SJW, TT, RK, DG, PR; Methodology, SJW, YN, TT, YS, JP, NM, RK; Validation, SJW, SK; Formal analysis, SJW; Investigation, SJW, SK, CZ, KOW, DP, HF, IH; Resources, RK, DG; Writing—Original Draft, SJW; Writing—Review & Editing, SJW, RK, DG, PR; Visualization, SJW; Supervision, RK, DG, PR; Funding Acquisition, SJW, PR.

Contrary to paradigm, SEC22B-deficient DCs efficiently cross-present both *in vivo* and *in vitro*. Though *in vitro* shRNA-mediated *Sec22b* silencing in bone marrow-derived dendritic cells (BMDCs) reduced cross-presentation, treatment of SEC22B-deficient BMDCs with the same shRNA produced a similar defect, suggesting the *Sec22b* shRNA modulates cross-presentation through off-target effects. RNAseq of *Sec22b* shRNA-treated SEC22B-deficient BMDCs demonstrated several changes in the transcriptome. Our data demonstrate that, contrary to the accepted model, that SEC22B is not necessary for cross-presentation, cautioning against extrapolating phenotypes from knockdown studies alone.

Graphical Abstract

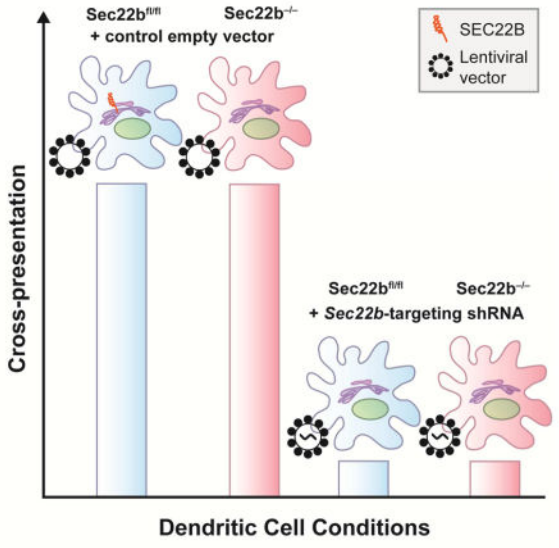

Introduction

Antigen cross-presentation describes the process by which exogenous antigen is processed and presented on MHC I to $CD8^+$ T cells (Joffre et al., 2012). Cross-presentation drives antigen-specific cytotoxic $CD8^+$ T cell responses against tumors and viruses lacking tropism for hematopoietic cells. Of the known antigen presenting cells, dendritic cells (DCs) are the most efficient cross-presenters (Banchereau and Steinman, 1998; Joffre et al., 2012).

The process of cross-presentation involves key steps that include (a) uptake of extracellular antigen, (b) processing of the antigen into peptides that can be presented on MHC I and (c) peptide-loading onto MHC I followed by trafficking of the MHC I:peptide complex to the surface of the cell. Disrupting any of these steps can alter cross-presentation (Joffre et al., 2012). At the antigen uptake stage, manipulation of endo- and phagocytic receptors modulates cross-presentation (Burgdorf et al., 2006; Gutierrez-Martinez et al., 2015; Mintern et al., 2015). Subsequent processing of internalized antigen is also highly regulated. For example, as endosomes and phagosomes mature, they acidify and proteolytic activity increases. Evidence suggests that delaying maturation and maintaining an elevated pH, a process mediated in part by NOX2 activity, regulated by Rac2 (Savina et al., 2006; Savina et

al., 2009) and Siglec-G-mediated signaling (Ding et al., 2016), promotes cross-presentation. The immunoproteasome has also been implicated at the antigen processing stage of cross-presentation (Palmowski et al., 2006). Additionally, loss of ERAP1, involved in the final peptide processing steps for loading onto MHC I, has been shown to be necessary for cross-presentation of cell-associated antigen and immune-complexed antigen (Firat et al., 2007). Finally, because cross-presenting MHC I may derive from the endoplasmic reticulum (ER) or from the cell surface through the endocytic recycling compartment (Adiko et al., 2015), trafficking of MHC I can impact cross-presentation efficiency as well(Nair-Gupta et al., 2014).

Notably, the events necessary for cross-presentation require resources from a wide array of cell compartments. Thus, to unify these distinct cell biological observations into a centralized antigen cross-presentation pathway, much attention has been given to intracellular trafficking pathways. SNARE proteins, which mediate vesicle fusion events, are essential for nearly all intracellular trafficking pathways (Chen and Scheller, 2001). Recently, the ER-SNARE protein SEC22B was identified as a key mediator of cross-presentation (Cebrian et al., 2011). SEC22B localizes to the ER-Golgi intermediate compartment (ERGIC) (Cebrian et al., 2011; Zhang et al., 1999) and interacts with plasma membrane-SNARE syntaxin 4 and Golgi-SNARE syntaxin 5 (Cebrian et al., 2011). Cebrian *et al* and others used an *in vitro* shRNA-mediated knockdown (KD) approach to reduce *Sec22b* expression in DCs, which resulted in increased access of antigen to the cytosol, delayed phagosomal maturation, increased access of ER-associated proteins to the phagosome, and ultimately reduced cross-presentation without affecting conventional antigen presentation pathways (Cebrian et al., 2011; Nair-Gupta et al., 2014). While its central regulatory role has been incorporated into the current model of cytosolic cross-presentation (Adiko et al., 2015; Blander, 2016; Blum et al., 2013; Gutierrez-Martinez et al., 2015; Joffre et al., 2012; Mantegazza et al., 2013; Mintern et al., 2015; Nair-Gupta and Blander, 2013; Schuette and Burgdorf, 2014; Segura and Amigorena, 2015), whether SEC22B is critical for antigen cross-presentation *in vivo* remains unknown.

Because DCs are the most efficient cross-presenting cells *in vivo*, we generated a DC-specific *Sec22b* knockout mouse (*CD11c-Cre Sec22b*$^{fl/fl}$) to address this outstanding question. Based on our understanding of SEC22B's function in DCs *in vitro*, we hypothesized SEC22B would be critical for cross-presentation *in vivo*. In contrast to the above reports, SEC22B did not regulate cross-presentation *in vivo*. Furthermore, analysis of *Sec22b*$^{-/-}$ DCs *in vitro* demonstrated no defect in cross-presentation across varying antigenic sources and lengths of incubation. However, treatment of *Sec22b*$^{-/-}$ BMDCs with the previously reported *Sec22b*-targeting shRNA recapitulated the cross-presentation defect. Furthermore, RNAseq analysis identified a reduction in mRNA transcripts for many off-target genes, demonstrating that the effect of KD on cross-presentation is independent of SEC22B. Taken together, our data demonstrate that, contrary to the current paradigm, SEC22B is not required for cross-presentation either *in vivo* or *in vitro*.

Results

DC-specific *Sec22b* knockout mice demonstrate normal immune cell composition and DC functions

We generated DC-specific *Sec22b* knockout mice by first breeding *Sec22b* gene-trapped mice (*Sec22b*^{cgt}) to *FLP* recombinase expressing mice to create *Sec22b*$^{fl/fl}$ mice (Figure 1A). *Sec22b*$^{fl/fl}$ (FL) mice were then bred to *CD11c-Cre* (*Itgax-Cre*) mice to generate *CD11c-Cre Sec22b*$^{fl/fl}$ (KO) mice where exon 3 of *Sec22b* is deleted specifically in CD11c-expressing DCs (Figure 1A). This excision event was confirmed by PCR (Figure 1B, C) using genomic DNA from MACS-enriched CD11c^{+} BMDCs (Figure S1A) and FACS-enriched CD11c^{+} CD8^{+} and CD8$^{−}$ splenic DCs (Figure S1B). Splenic DCs from *CD11c-Cre Sec22b*$^{fl/fl}$ mice exhibited virtually complete *Sec22b* knockout (Figure 1B, C) and a majority of BMDCs from these mice had also undergone Cre-mediated excision at exon 3 (Figure 1B, C). Loss of *Sec22b* expression was confirmed by qRT-PCR (Figure 1D) and Western Blot (Figure 1E, F) analysis with marked reduction of *Sec22b* in CD11c^{+} BMDCs (Figure 1D, E, F) and splenic DCs (Figure 1E, F).

Next, we assessed the impact of SEC22B-deficiency in CD11c^{+} cells on DC development, phenotype, and the development of other immune cells. We immunophenotyped *CD11c-Cre Sec22b*$^{fl/fl}$ mice and observed normal development of DC and myeloid cell populations (Figure 1G, S2A), T cell populations (Figure S2B), thymocyte differentiation (Figure S2C), T cell activation state (Figure S2D), and other lymphoid populations (Figure S2E).

We then determined whether absence of SEC22B affects DC functions. We first tested *Sec22b*$^{−/−}$ BMDC responses to innate immune stimuli by overnight culture of MACS-enriched CD11c^{+} BMDCs (Figure S1A) with TLR 1/2, 2, and 4 ligands Pam3CSK, peptidoglycan, and LPS, respectively. Supernatants were tested by ELISA for production of TNFα and IL-12, which did not differ between *CD11c-Cre Sec22b*$^{fl/fl}$ and *CD11c-WT Sec22b*$^{fl/fl}$ samples (Figure 1H). To determine direct antigen presentation capability, we assessed MHC surface expression on MACS-enriched CD11c^{+} splenic DCs (Figure S1C) from *CD11c-Cre Sec22b*$^{fl/fl}$ or *CD11c-WT Sec22b*$^{fl/fl}$ animals, using them as stimulators in an allogeneic mixed lymphocyte reaction. After 4 days of incubation, allogeneic BALB/c T cell proliferation was measured by ^{3}H-thymidine uptake and found to be similar between stimulation groups (Figure 1I). Finally, we tested the impact of SEC22B on antigen uptake. We incubated MACS-enriched CD11c^{+} *Sec22b*$^{−/−}$ BMDCs (Figure S1A) with FITC-dextran for 30 minutes at either 4°C or 37°C. BMDCs that had taken up antigen (CD11c^{+} FITC^{+} cells) were identified by flow cytometry. We observed no dependence on SEC22B expression for antigen uptake (Figure 1J). Taken together, these data suggest SEC22B is dispensable for DC development, cytokine response to TLR stimulation, direct antigen presentation, and endocytic antigen uptake.

Cross-presentation *in vivo* does not rely on SEC22B expression in dendritic cells

We next analyzed whether SEC22B expression in DCs is required for *in vivo* cross-presentation. In light of previous data (Cebrian et al., 2011; Nair-Gupta et al., 2014), we hypothesized that the absence of SEC22B would reduce cross-presentation. We performed

an *in vivo* cross-presentation assay as described previously (Kool et al., 2008). Briefly, we intraperitoneally (i.p.) injected ovalbumin (OVA) antigen or bovine serum albumin (BSA), then adoptively transferred CFSE-stained OT-I T cells. After 7 days, spleen, mesenteric lymph nodes (mLN), and the superficial inguinal lymph nodes from the side ipsilateral to antigen administration (siLN) were harvested and analyzed by flow cytometry for proliferation of SIINFEKL ($OVA_{257–264}$)-restricted $CD8^+$ T cells (OT-I T cells) (Figure 2A, B). Surprisingly, animals lacking SEC22B in $CD11c^+$ cells induced robust proliferation of OT-I T cells (Figure 2B, C). Indeed, comparing *CD11c-Cre Sec22b*$^{fl/fl}$ or *CD11c-WT Sec22b*$^{fl/fl}$ mice, we observed no differences in the proliferation of OVA-specific T cells. These data demonstrate that SEC22B is not required for *in vivo* cross-presentation of soluble antigens.

SEC22B is not necessary for cross-presentation of soluble or particulate antigen *in vitro*

Because our *in vivo* results appeared to contradict previous observations on the role of SEC22B in cross-presentation (Cebrian et al., 2011; Nair-Gupta et al., 2014), we wanted to test the possibility that SEC22B regulation of cross-presentation may only be germane to *in vitro* studies. To do this, we used MACS-enriched $CD11c^+$ splenic DCs (Figure S1C) to cross-present soluble OVA to OT-I T cells under the same conditions used in the cited reports. However, *Sec22b*$^{-/-}$ splenic DCs induced similar OT-I T cell proliferation and expression of activation markers as compared to control DCs (Figure 3A, B). The use of the SIINFEKL control peptide, which can be presented by the MHC I molecule H2-K^b without further processing, verified that MHC I expression on the BMDCs was not perturbed (Figure 3A, B). Similar results were obtained with MACS-enriched $CD11c^+$ *Sec22b*$^{-/-}$ BMDCs (Figure S1A), demonstrating that SEC22B does not have a unique regulatory function in BMDCs compared to splenic DCs (Figure 3C, Figure S3).

To confirm that antigen type is not a critical determinant for SEC22B regulation of cross-presentation in DCs, we analyzed the ability of *Sec22b*$^{-/-}$ BMDCs to cross-present particulate antigen. Using OVA-coated latex beads, we found cross-presentation of particulate antigen to be independent of SEC22B expression (Figure 3D, E, S3). Beads were efficiently excluded by their scatter plot distribution (Figure 3F) and thus did not confound analysis. We excluded the possibility that OVA source or endotoxin contamination was confounding our data by testing *Sec22b*$^{-/-}$ BMDCs with endotoxin-free OVA from a different supplier, which failed to produce a cross-presentation defect (Figure S4). We therefore conclude that SEC22B is not required for cross-presentation of soluble or particulate antigen.

shRNA-mediated knockdown of *Sec22b* reduces cross-presentation in BMDCs

SEC22B was previously identified as a cross-presentation mediator using shRNA to silence its expression in BMDCs (Cebrian et al., 2011; Nair-Gupta et al., 2014). Our discrepant observations might then be secondary to methodology, i.e. potential differences between a genetic knockout approach versus a molecular silencing approach. To corroborate this, we obtained a previously validated shRNA sequence (Cebrian et al., 2011), shRNA 90, to silence *Sec22b in vitro* in BMDCs generated from C57/BL6 (WT) mice (Figure 4A). Using previously reported conditions (Cebrian et al., 2011; Nair-Gupta et al., 2014), we

administered soluble OVA to shRNA-treated BMDCs and measured cross-presentation with CFSE-stained OT-I T cells. Consistent with previous observations (Cebrian et al., 2011; Nair-Gupta et al., 2014), we observed that *Sec22b* KD BMDCs showed reduced cross-presentation of OVA when compared with BMDCs treated with an empty vector (EV) control (Figure 4B, C). Thus, shRNA-mediated KD of Sec22b reduces cross-presentation, as previously demonstrated (Cebrian et al., 2011; Nair-Gupta et al., 2014).

Sec22b-targeting shRNAs 89 and 90 mediate cross-presentation through effects on off-target genes

Collectively, our observations demonstrate when *Sec22b* is knocked out, it is not necessary for cross-presentation (Figures 2B, C, 3, S3, 4), but when knocked down in BMDCs, it seems to be essential (Cebrian et al., 2011; Nair-Gupta et al., 2014) (Figure 4B, C).

To resolve the discrepancy between the knockout and KD results, we systematically analyzed three potentially mutually exclusive hypotheses: (1) there is compensation by other *Sec22* paralogs for the loss of SEC22B only in the total absence of *Sec22b* (in *CD11c-Cre* $Sec22b^{fl/fl}$ mice or $Sec22b^{-/-}$ DCs), but not in an acute deficiency state (in *Sec22b* KD BMDCs), a confounding possibility observed in another model system (Rossi et al., 2015); (2) viral stimulation and silenced *Sec22b* expression together reduce cross-presentation, suggesting that viral infection might have uniquely induced predominant use of a SEC22B-dependent cross-presentation system; or (3) the observed effects of the shRNA on cross-presentation may be a consequence of off-target effects of the shRNA.

In mammals, there are two *Sec22b* paralogs, *Sec22a* and *Sec22c* (Zhang et al., 1999). While little is known about the functions of SEC22A and C, they have been shown to localize to the ER (Tang et al., 1998; Zhang et al., 1999), and so might plausibly compensate for loss of SEC22B. To test this, we quantified *Sec22a* and *Sec22c* transcripts in MACS-enriched $CD11c^{+}$ $Sec22b^{-/-}$ and $Sec22b^{fl/fl}$ BMDCs. If SEC22A and/or SEC22C were functionally compensating for loss of SEC22B, we hypothesized we would see an increase in expression of these genes in $Sec22b^{-/-}$ DCs. Using qRT-PCR, we observed no difference in the level of *Sec22a* or *Sec22c* expression relative to housekeeping gene *Gapdh* in $Sec22b^{-/-}$ BMDCs compared to $Sec22b^{fl/fl}$ controls (Figure S5). These data suggest that the absence of a cross-presentation defect in $Sec22b^{-/-}$ DCs is not likely due to compensation by paralogs.

Next, to clearly distinguish between the remaining two possibilities, we performed the following experiment. We transduced $Sec22b^{-/-}$ and $Sec22b^{fl/fl}$ BMDCs with shRNA 90 or EV control (Figure 5A, B). After each BMDC group was incubated with soluble OVA, washed, fixed, and cultured with CFSE-stained OT-I T cells, we observed deficient cross-presentation in all groups treated with shRNA 90, independent of *Sec22b* genotype (Figure 5C). These data suggested that shRNA 90 mediates its effects on cross-presentation not through its activity on *Sec22b* but through off-target effects (hypothesis 3).Additionally, these data further invalidate the idea that there may be functional compensation for the loss of SEC22B (hypothesis 1), because, were that the case, cross-presentation would have been reduced only in the shRNA 90-treated $Sec22b^{fl/fl}$ BMDC (FL+90) condition. Furthermore, this data also invalidates the hypothesis that viral stimulation uniquely activates a Sec22b-dependent cross-presentation pathway (hypothesis 2). Such a phenomenon would have

resulted in reduced cross-presentation in all conditions where there was loss of Sec22b expression (FL+90, KO+EV, KO+90). Collectively, these data strongly suggest that shRNA 90 reduces cross-presentation in BMDCs through its off-target effects.

Although our data demonstrate shRNA 90 alters cross-presentation through secondary effects on non-*Sec22b* genes, others have published observations on SEC22B and cross-presentation using a different shRNA sequence, shRNA 89 (Nair-Gupta et al., 2014). Examining shRNAs 89 and 90, we noted an 8 nucleotide overlap in the gene-targeting regions of both shRNAs (5′-CCCTATTC-3′). In fact, these two shRNA sequences target the same segment of *Sec22b* exon 3. We wondered if shRNA 89 also mediates its effects on cross-presentation by silencing off-target genes. To address this, we treated $Sec22b^{-/-}$ BMDCs with shRNA 89 (Figure 5A, B) and again observed a reduction in cross-presentation (Figure 5D), similar to shRNA 90.

Based on these data, we reasoned that the cross-presentation defect previously attributed to *Sec22b* silencing by shRNA-mediated knockdown (KD) was likely due to silencing of at least one off-target gene by shRNA 89 and 90. To test this, we rescued SEC22B expression in $Sec22b^{-/-}$ BMDCs treated with shRNA 90 using an overexpression vector to express a *Sec22b* transgene with silent mutations at the shRNA 89 and 90 binding site ($Sec22b^{\Delta}$) (Figure 5E–G). Viable, $CD11c^{+}$ GFP+ cells ($Sec22b^{\Delta}$-expressing, shRNA 90-transduced, BMDCs) were enriched by FACS (Figure S1D). The rescue of SEC22B expression by $Sec22b^{\Delta}$ had no effect on cross-presentation (Figure 5H). This further demonstrates cross-presentation is independent of SEC22B and that the impact of shRNA 89 and 90 treatment on cross-presentation is mediated through off-target effects.

To formally test for evidence of off-target effects on gene expression, we used RNAseq to determine whether the utilization of these shRNAs altered RNA transcript levels of genes other than *Sec22b*. We assessed differential gene expression in $Sec22b^{-/-}$ BMDCs in response to shRNA 89 and 90 treatment compared to EV treatment (Figure 5I). We identified over 20 genes that were highly expressed in EV controls but whose expression was significantly downregulated (q-value<0.05) under both shRNA 89 and 90 treatment conditions (Figure 5J). Taken together, these data confirm that shRNA 89 and 90 target an overlapping set of off-target genes and suggest these off-target effects reduce cross-presentation by BMDCs.

Discussion

Part of the current cross-presentation paradigm includes a critical regulatory role for SEC22B (Adiko et al., 2015; Blander, 2016; Blum et al., 2013; Gutierrez-Martinez et al., 2015; Joffre et al., 2012; Mantegazza et al., 2013; Mintern et al., 2015; Nair-Gupta and Blander, 2013; Schuette and Burgdorf, 2014; Segura and Amigorena, 2015). However, this understanding was based primarily on *in vitro* studies (Cebrian et al., 2011; Nair-Gupta et al., 2014) and had never been confirmed *in vivo*. Thus, we began this study seeking to answer this outstanding question: does SEC22B play a crucial role in cross-presentation *in vivo*? Utilizing a *CD11c-Cre* $Sec22b^{fl/fl}$ mouse to specifically delete *Sec22b* in DCs, we discovered that SEC22B is dispensable for *in vivo* antigen cross-presentation (Figure 2B, C).

Furthermore, challenging the current paradigm, using soluble (Figure 3A, B, C, S3, S4) and particulate (Figure 3D, E, S3, S4) OVA model antigen, we also found that Sec22b was not necessary for cross-presentation *in vitro*. We observed no distinction between DC sources; both CD11c^{+} *Sec22b*$^{-/-}$ splenic DCs (Figure 3A, B) and CD11c^{+} *Sec22b*$^{-/-}$ BMDCs (Figure 3C, D, E, Figure S3) were fully competent cross-presenters thus ruling out tissue- and culture-specific artifacts as potential confounders.

Genetic deletion of *Sec22b* thus produced data that posed a seeming contradiction to data obtained from BMDCs with shRNA-mediated *Sec22b* KD (Cebrian et al., 2011; Nair-Gupta et al., 2014). Notably, treatment of BMDCs with the same shRNA sequences reduced cross-presentation in both *Sec22b*$^{-/-}$ and *Sec22b*$^{fl/fl}$ BMDCs (Figure 5C, D). This data demonstrate the cross-presentation defect previously associated with *Sec22b* silencing is instead linked to treatment with shRNA containing the nucleotide sequence 5′-CCCTATTC-3′, targeting the 3rd exon of *Sec22b*. These data were further bolstered by rescue of SEC22B expression in KD BMDCs (Figure 5E–G), which failed to rescue the shRNA-induced cross-presentation defect (Figure 5H), and by RNA sequencing of EV- and shRNA-treated KO BMDCs, which identified over 20 other unique targets of the *Sec22b*-“specific” shRNAs used (Figure 5J).

These collective findings serve to clarify the common understanding that SEC22B is essential for cross-presentation (Adiko et al., 2015; Blander, 2016; Blum et al., 2013; Gutierrez-Martinez et al., 2015; Joffre et al., 2012; Mantegazza et al., 2013; Mintern et al., 2015; Nair-Gupta and Blander, 2013; Schuette and Burgdorf, 2014; Segura and Amigorena, 2015). While our data confirms Cebrian et al’s finding that KD with shRNA 90 does indeed reduce cross-presentation, it also suggests the cross-presentation phenotype was misattributed to *Sec22b* silencing.

A potential caveat to our studies might be found in the residual SEC22B expression seen in the *CD11c-Cre Sec22b*$^{fl/fl}$ BMDCs (Figure 1B–F). Cre-mediated excision of exon 3 in this population was 66% efficient (Figure 1C), which might be due to either mosaic Cre expression amongst DCs or inefficient Cre activity. It is thus theoretically possible that a fraction of SEC22B-producing DCs in the KO condition are capable of cross-presenting to T cells as efficiently as the entire population of DCs in the FL condition. However, the uniform response to antigen dose, almost complete loss of SEC22B protein in CD11c^{+} BMDCs obtained from *CD11c-Cre Sec22b*$^{fl/fl}$ mice (Figure 1E, F), and the inability of *Sec22b*$^{\Delta}$ rescue (Figure 5E–G) to mitigate the shRNA 90-induced cross-presentation defect (Figure 5H) suggest that this is an unlikely event. Additional investigation will be needed to explore what impacts SEC22B overexpression in wildtype cells may have on cross-presentation, as our data do not address this.

In summary, our data do not exclude a role for SEC22B in cross-presentation but do demonstrate that SEC22B cannot be considered to be required for cross-presentation of soluble or particulate antigens. Further work will be necessary to determine the role of SEC22B in the cross-presentation of cell-associated antigens.

Our findings, moreover, offer an opportunity to identify which factor(s) is/are truly responsible for the cross-presentation defect induced by *Sec22b* shRNAs 89 and 90. Many of the off-target genes identified (Figure 5J) have no known association with antigen presentation pathways, though several do. Several protein products of the many genes that were altered are involved in phagosomal biology (Alloatti et al., 2015), cell-trafficking and immune-regulation. Notably, our inability to identify a single obvious off-target gene leaves open the possibility that shRNAs 89 and 90 mediate their effects on cross-presentation through the knockdown of several genes, which may function in an integrative fashion to promote cross-presentation.

For the wider community of experimental biologists using molecular techniques to manipulate gene expression, our data offers a cautionary tale. RNAi technology carries the risk of off-target effects (Jackson et al., 2003; Jackson and Linsley, 2004; Scacheri et al., 2004; Snove and Holen, 2004). The off-target problem is not exclusive to KD technologies as the same concerns have been noted with endonuclease-mediated genome editing techniques (Fu et al., 2013; Hendel et al., 2015; Hsu et al., 2013; Koo et al., 2015; Pattanayak et al., 2013). Nor is this limited to mammalian systems. An elegant study in zebrafish found that 80% of phenotypes observed using morpholino-mediated silencing could not be replicated in knockout models (Kok et al., 2015). Thus, our data support validation of gene targets with multiple methodologies as any one approach carries significant limitations.

Our findings correct the field's understanding of SEC22B's role in cross-presentation using a DC-specific *Sec22b* knockout mouse to demonstrate that there is no dependence on SEC22B expression for efficient cross-presentation. While this appears to contradict the observation that shRNA-mediated knockdown of *Sec22b* reduces cross-presentation efficiency, our data show the observed cross-presentation defect is likely due to the shRNA sequences acting on off-target genes. Taken together, our findings also point to the possibility of other potentially novel critical mediator(s) of cross-presentation.

Experimental Procedures

Reagents

RPMI, penicillin and streptomycin, and sodium pyruvate were purchased from Gibco; FCS from GemCell and Gemini, 2-ME from Sigma-Aldrich. Lipopolysaccharide (tlrl-smlps), Pam3CSK4 (tlrl-pms), and peptidoglycan (tlrl-pgns2) were obtained from Invivogen. Ovalbumin (OVA, A5503) and SIINFEKL/$OVA_{257–264}$ (S7951) antigen were purchased from Sigma-Aldrich unless otherwise noted. Bovine serum albumin (BSA, BP1600) was purchased from FisherScientific.

Mice

C57BL/6 (027) and Balb/c (028) wildtype mice were obtained from Charles River Laboratories. Two OT-I mouse models were used based on availability of reagents. OT-I transgenic TCR mice were obtained from Jackson Laboratory (003831) and *Rag2* KO OT-I mice were obtained from Taconic (2334). *Sec22b* gene-trapped founder mice were obtained

from the European Conditional Mouse Mutagenesis Program (EUCOMM; Sec22b$^{tm1a(EUCOMM)Wtsi}$) and bred to *FLP* recombinase mice (005703, The Jackson Laboratory) to excise the *FRT*-flanked region between exons 2 and 3 (Figure 1A) and generate *Sec22b$^{fl/fl}$* mice (Figure 1A). *CD11c-Cre* transgenic mice (008068, The Jackson Laboratory) were then bred to *Sec22b$^{fl/fl}$* mice to create *CD11c-Cre Sec22b$^{fl/fl}$* mice. Mice used for experiments ranged between 8 weeks and 1 year old and included both males and females. All animals were cared for under regulations reviewed and approved by the University Committee on Use and Care of Animals of the University of Michigan, based on University Laboratory Animal Medicine guidelines.

Genotyping—The following primers were used to genotype the *Sec22b* allele: 5′-AAGGGTGGATGGATTCTTCACAC-3′ (*Sec22b* F1), 5′-TTGGTGGCCTGTCCCTCTCACCTT-3′ (*Sec22b* B1), 5′-GCAGCTCAGCAGTAAGAACACGTC-3′ (*Sec22b* B2). The *Sec22b* F1+B1 primer pair was used to identify gene-trapped mice and the *Sec22b* F1+B2 primer pair was used to identify *floxed* mice. *Cre* primer sequences were: 5′-TTACCGGTCGATGCAACGAGT-3′ (*Cre* F) and 5′-TTCCATGAGTGAACGAACCTGG-3′ (*Cre* R).

Cells

Loosely adherent and nonadherent BMDCs were harvested after 7 days of bone marrow cell culture in GM-CSF (20 ng/mL, Peprotech, 315-03)-containing media. Where indicated, BMDCs were enriched with CD11c UltraPure MicroBeads (Miltenyi, 130-108-338) by MACS sorting. To obtain splenic DCs, spleens were cut into thirds, flushed with 1 mg/mL collagense D (Roche, 11088866001) and incubated for 1 hr at 37°C. Digested spleens were then homogenized between frosted slides, filtered through a 40 um cell strainer to achieve a single-cell suspension, and enriched with CD11c UltraPure MicroBeads. T cells were isolated from single cell homogenates from spleen and lymph nodes and isolated using CD90.2 MicroBeads (Miltenyi, 130-049-101).

Flow cytometry

Antibodies—All antibodies were obtained from eBioscience and BioLegend: CD3 (145-2C11), CD4 (GK1.5), CD8α (53-6.7), CCR7 (4B12), CD62L (MEL-14), CD44 (IM7), CD69 (H1.2F3), CD25 (3C7), IL-2 (JES6-5H4), IFNγ (XMG1.2), CD11c (N418), CD11b (M1/70), CD205 (NLDC-145), F4/80 (BM8), B220/CD45R (RA3-6B2), NK1.1 (PK136), TCRβ (H57-597), TCRγδ (GL3), I-A/I-E (M5/114.15.2), Annexin V-APC (BioLegend, 640920), 7-AAD (BioLegend, 420404). H-2Kb OVA-APC (T03002) and H2-Kb LCMV-APC (T03019) tetramers were purchased from MBL International Corporation.

Cell staining—For immunophenotyping, single-cell suspensions were obtained by homogenizing tissues between frosted glass slides then filtering homogenates through a 40 um cell strainer. OT-I T cells were stained with 5 uM CFSE (Invitrogen, C34554) according to manufacturer's protocol. To control for nonspecific binding, cells were blocked with anti-CD16/CD32 antibody (BD Biosciences, 2.4G2) for 10 minutes at room temperature. Tetramer staining was performed according to manufacturer's protocol.

Surface staining for flow analysis was performed at 0.5 μL antibody/test for 15 minutes at 4°C, protected from light. For surface s taining for flow sorting, cells were resuspended at 5×10^6 cells/mL with 5 μL/mL antibody for 30 minutes at 4°C. Cells were fixed and any red blood cells lysed in Fix/Lyse solution (BD Biosciences, 349202) according to manufacturer's instructions.

For intracellular staining, cells were stimulated with PMA/ionomycin (eBioscience, 00-4975) and treated with brefeldin A (eBioscience, 00-4506-5) for 5 hours at 37°C. Permeabilization buffer (eBioscience, 00-8333) was used for intracellular cytokine staining which was performed at 0.5 uL antibody/test for 30 minutes at room temperature, protected from light.

Flow analysis—Cells were run on an Accuri C6, MACSQuant Analyzer, BioRad ZE5 Cell Analyzer, or Attune NxT. All analysis was performed using FlowJo v10.2.

Cell sorting—BMDCs were prepared for sorting by resuspending in FACS buffer containing 5 mM EDTA (Lonza, 51201) to prevent cell aggregation. Cells were sorted on a Beckman Coulter MoFlo Astrios EQ, Sony SY3200, or BD FACSAria II.

Western Blots

Whole cell lysates were obtained and protein concentrations determined by BCA Protein Assay (Thermo Scientific, 23225). Protein was separated by SDS-PAGE gel electrophoresis and transferred to PVDF membrane (Millipore, IPVH00010) using a Bio-Rad semi-dry transfer cell (1703940) (20V, 1h). Blots were incubated with SEC22B (1:200, Santa Cruz, 29-F7) and B-ACTIN (1:1000, abcam, ab8226) primary antibodies overnight at 4°C. Incubation with secondary anti-mo use antibody conjugated to HRP (1:10,000, Santa Cruz, sc-2005) was performed for 1 hour at room temperature. Bound antibody was revealed using SuperSignal ECL substrate (Thermo Scientific). Densitometric analysis was performed using ImageJ.

Mixed lymphocyte reaction

5000 MACS-sorted $CD11c^+$ splenic cells were cultured with 2×10^5 CD90.2+ T cells from Balb/c or C57BL/6 mice 96 well flat-bottom plates in 200 uL media for 96 hours. Incorporation of ^{3}H-thymidine (1 μCi/well) by proliferating T cells during the final 7 hours of culture was measured by a TopCount NXT (PerkinElmer, C9902).

ELISA

Supernatants from cell culture were harvested and analyzed for IL-12 (BD Biosciences, 555240) and TNFα (R&D Systems, MTA00B) following manufacturer's instructions.

Antigen Presentation Assays

In vitro cross-presentation of soluble OVA—DCs were plated at 0.05×10^6 cells/well or 0.025×10^6 cells/well for rescue assays in 96 well flat-bottom plates and incubated with OVA or SIINFEKL dissolved in 1xPBS for 2 hours at 37°C, unless otherwise noted. Cells were t hen washed with 1xPBS and fixed with 1% formaldehyde. Fixation was quenched by

0.2M glycine (Sigma-Aldrich, G5417) solution after which 0.2×10^6/well CFSE-stained OT-I T cells were added. Assays were harvested 72 hours later.

In vitro cross-presentation of bead-bound OVA—OVA and/or BSA was attached to 3 um carboxylate microspheres (Polysciences, 09850-5) using passive adsorption. Differing ratios of OVA to BSA were used (100% OVA/0% BSA, 33% OVA/66% BSA, and 0% OVA/100% BSA) to achieve a dose response. Beads were washed in MES buffer (Thermo Scientific, 28390) resuspended at 2% solids, then incubated with antigen (10 mg/mL total) overnight at room temperature with gentle rocking. Beads were washed 3 times in MES buffer then stored at 1% solids in 1xPBS+0.1% glycine at 4°C until use. 1×10^6 beads were incubated with 0.1×10^6 MACS-sorted $CD11c^+$ BMDCs for 2 hours at 37°C. Subsequently, DCs were processed as in the soluble OVA cross-presentation assay.

In vivo cross-presentation assays—As previously described (Kool et al., 2008), on day 0, OVA or BSA was injected *i.p.* and 10×10^6 CFSE-stained OT-I T cells were delivered *i.v.* On day 7, spleen, mesenteric lymph nodes, and superficial inguinal lymph nodes ipsilateral to the side of antigen administration were harvested, processed, and analyzed by flow cytometry for SIINFEKL-restricted CD3+ CD8+ T cell proliferation from cross-presentation.

Excision PCR

Genomic DNA was purified from MACS sorted BMDCs and FACS sorted splenic DCs using Trizol LS (Invitrogen, 10296028) according to manufacturer's instructions. The following primers and GoTaq Green Master Mix (Promega, M7122) were used to detect alleles: *Sec22b* F1, 5′-TCCTTTTGAATGGAGAAAGCTTC-3′ (F2), and 5′-CCTGTGACAGTCTACAGATTGGA-3′ (R). All reactions were performed according to manufacturer's instructions. 1 Kb Plus DNA Ladder (ThermoFisher, 10787018) was used for agarose gel analysis.

Quantitative RT-PCR

Cells were homogenized using a Qiagen QIAshredder (79654) and RNA purified using a Qiagen RNeasy Mini Kit (74104). Using SuperScript VILO (Invitrogen, 11754050), mRNA was reverse-transcribed into cDNA. The following primers and SYBR green (PowerUP SYBR Green Master Mix, Applied Biosystems, A25742) were used to detect transcripts: 5′-CAGGGCTCTAGACCCAAGTAGCA-3′ and 5′-CCAGTGCTGTGCCACCATGAAA-3′ (Sec22a), 5′-GCTCGGAGAAATCTAGGCTCC-3′ and 5′-CCCCGCTGTAGGACTTCTTC-3′ (Sec22b), 5′-GGGCGAGGTGTCCCCATGAC-3′ and 5′-AGGCTGAGAGGGGCAGTCCA-3′ (Sec22c), 5′-TGACCTCAACTACATGGTCTACA-3′ and 5′-CTTCCCATTCTCGGCCTTG-3′ (GAPDH). All reactions were performed according to manufacturer's instructions. The specificity of each reaction was verified by agarose gel analysis.

Lentiviral shRNA Knockdown and Overexpression of Sec22b

Generation of shRNA plasmids—RNA Consortium plasmids encoding shRNA-expressing lentivirus (TRCN0000115089 (89), TRCN0000115090 (90)) were obtained from

ThermoFisher. Empty vector (EV, 10879) plasmid was obtained from Addgene. Plasmids were transformed into JM109 competent cells (P9751, Promega) following manufacturer's instructions. Preps were purified for lentiviral generation using the Qiagen Plasmid Plus Midi Kit (12943).

Generation of Sec22b$^{\Delta}$ transgene overexpression vector—Total RNA was prepared using Trizol LS according to manufacturer's instructions. SuperScript IV (Invitrogen, 18090010) was used to generate cDNA. *Sec22b* was amplified and adapted for TOPO cloning using AccuPrime Pfx Polymerase (Invitrogen, 12344024) and 5′-CACCATGGTGCTGCTGACGAT-3′ and 5′-TCACAGCCACCAAAACCGCA-3′ primers. Reaction products were analyzed by electrophoresis, then were gel purified (Qiagen Gel Extraction Kit, 28104), ligated to TOPO vector (Invitrogen, K2400-200) following manufacturer's instructions, and transformed into TOP10 chemically competent cells (Invitrogen, C404010). Site-directed mutagenesis was performed using AccuPrime Pfx Polymerase and 5′-TACAGTTTTATTGAGTTTGATACCTTCATTCAGAAA-3′ and 5′-TGGACGGCTAACAG TGGGCACCTTCTTC-3′ primers in order to induce silent mutations at the site of shRNA 89 and 90 binding. Gateway™ recombination was used to insert the transgene into expression vector pLenti7.3/V5-DEST™ (Invitrogen, V53406). Clones were sequenced to verify sequences and in-frame insertion and plasmids from amplified preps were purified for lentiviral generation using the Qiagen Plasmid Plus Midi Kit (12943).

Generation of lentivirus—Plasmids were packaged using HEK293T cells by the University of Michigan Medical School Vector Core using a VSV-G envelope. Supernatants containing viral particles were concentrated 10X.

Dendritic cell infection—Bone marrow was plated in GM-CSF-containing media at 5×10^6 cells per 100 mm dish on day 0. On day 2, cells were infected with 0.5 mL 10X shRNA-containing virus and, where indicated, 1 mL 10X *Sec22b*$^{\Delta}$-containing virus in a total of 5 mL GM-CSF-containing media with polybrene (8 ug/mL, Sigma-Aldrich, 107689). On day 4, cells treated with EV or shRNA 89 or 90 were selected with puromycin (5 ug/mL, Sigma-Aldrich, P8833) in 10 mL GM-CSF containing media. On day 7, BMDCs were harvested for assay use.

RNA-Seq

RNA preparation and sequencing—Total RNA was prepared using Trizol LS according to manufacturer's instructions and assessed for quality using a TapeStation (Agilent, Santa Clara, CA) following manufacturer's recommendations. Samples with RNA integrity numbers of 8 or greater were prepped using the Illumina TruSeq Stranded mRNA Library Prep kit (RS-122-2101, RS-122-2102) (Illumina, San Diego, CA) using manufacturer's recommended protocols, where 1ug of total RNA was ribo-depleted with Epicentre Ribo-Zero protocol. Depleted RNA was fragmented and copied into first strand cDNA using random primers. The 3′ ends of the cDNA were adenylated for ligation of adapters, one of which contained a 6-nucleotide barcode unique to each sample allowing for sample pooling. The products were purified and enriched by PCR to create the final cDNA

library. Final libraries were checked for quality and quantity by a TapeStation (Agilent) and qPCR using Kapa's library quantification kit for Illumina Sequencing platforms (KK4835) (Kapa Biosystems,Wilmington MA) using manufacturer's recommended protocols. Libraries were clustered on the cBot (Illumina) and sequenced 3 samples per lane on a 50 cycle paired end on a HiSeq 2500 (Illumina) in High Output mode using version 4 reagents according to manufacturer's recommended protocols.

Data Processing—RNA-sequencing reads were quantified to the mouse transcriptome (GENCODE vM4) using Kallisto (v0.43.0) (Bray et al., 2016). GENCODE vM4 GTF was obtained from GENCODE (https://www.gencodegenes.org/mouse_releases/4.html), and transcriptome fasta file was produced using the *rsem-prepare-reference* function of RSEM (version 1.2.26) (Li and Dewey, 2011). Kallisto index was generated using the *kallisto index* function. Transcript level quantification obtained using the *kallisto quant* function. Gene level expression obtained by summing the TPM values for all transcripts within each gene.

RNA-Seq Differential Expression Testing—Differentially expressed genes were obtained by comparing the shRNA 89 condition to empty vector and the shRNA 90 condition to empty vector using DESeq2 (Love et al., 2014). In order to detect the most robust loss of expression, only genes with mean expression of 20 TPM or greater in the empty vector condition were considered for analysis of downregulation. Significantly differentially expressed genes were defined as genes with a q-value<0.05.

Statistics

Unless otherwise noted, all statistical comparisons were performed using a 2-tailed unpaired t-test. Statistical significance was determined using the Holm-Sidak method, with alpha=0.05. Each condition was analyzed individually, without assuming a consistent SD. Further information on statistical analyses can be found in the figure legends for each experiment.

Supplementary Material

Refer to Web version on PubMed Central for supplementary material.

Acknowledgments

This work was supported by the US National Institutes of Health (NIH) grants HL-128046, HL-090775, CA-173878, CA-203542 and the Herman and Dorothy Miller Fund. We acknowledge use of the Vector Core, Flow Cytometry Core, and DNA Sequencing Core of the University of Michigan's Biomedical Research Core Facilities for preparation of reagents, use of equipment, processing of samples, and generation of data.

References

Adiko AC, Babdor J, Gutierrez-Martinez E, Guermonprez P, Saveanu L. Intracellular Transport Routes for MHC I and Their Relevance for Antigen Cross-Presentation. Front Immunol. 2015; 6:335. [PubMed: 26191062]

Alloatti A, Kotsias F, Pauwels AM, Carpier JM, Jouve M, Timmerman E, Pace L, Vargas P, Maurin M, Gehrmann U, et al. Toll-like Receptor 4 Engagement on Dendritic Cells Restrains Phago-Lysosome Fusion and Promotes Cross-Presentation of Antigens. Immunity. 2015; 43:1087–1100. [PubMed: 26682983]

Banchereau J, Steinman RM. Dendritic cells and the control of immunity. Nature. 1998; 392:245–252. [PubMed: 9521319]

Blander JM. The comings and goings of MHC class I molecules herald a new dawn in cross-presentation. Immunol Rev. 2016; 272:65–79. [PubMed: 27319343]

Blum JS, Wearsch PA, Cresswell P. Pathways of antigen processing. Annu Rev Immunol. 2013; 31:443–473. [PubMed: 23298205]

Bray NL, Pimentel H, Melsted P, Pachter L. Near-optimal probabilistic RNA-seq quantification. Nat Biotechnol. 2016; 34:525–527. [PubMed: 27043002]

Burgdorf S, Lukacs-Kornek V, Kurts C. The mannose receptor mediates uptake of soluble but not of cell-associated antigen for cross-presentation. J Immunol. 2006; 176:6770–6776. [PubMed: 16709836]

Cebrian I, Visentin G, Blanchard N, Jouve M, Bobard A, Moita C, Enninga J, Moita LF, Amigorena S, Savina A. Sec22b regulates phagosomal maturation and antigen crosspresentation by dendritic cells. Cell. 2011; 147:1355–1368. [PubMed: 22153078]

Chen YA, Scheller RH. SNARE-mediated membrane fusion. Nat Rev Mol Cell Biol. 2001; 2:98–106. [PubMed: 11252968]

Ding Y, Guo Z, Liu Y, Li X, Zhang Q, Xu X, Gu Y, Zhang Y, Zhao D, Cao X. The lectin Siglec-G inhibits dendritic cell cross-presentation by impairing MHC class I-peptide complex formation. Nat Immunol. 2016; 17:1167–1175. [PubMed: 27548433]

Firat E, Saveanu L, Aichele P, Staeheli P, Huai J, Gaedicke S, Nil A, Besin G, Kanzler B, van Endert P, et al. The role of endoplasmic reticulum-associated aminopeptidase 1 in immunity to infection and in cross-presentation. J Immunol. 2007; 178:2241–2248. [PubMed: 17277129]

Fu Y, Foden JA, Khayter C, Maeder ML, Reyon D, Joung JK, Sander JD. High-frequency off-target mutagenesis induced by CRISPR-Cas nucleases in human cells. Nat Biotechnol. 2013; 31:822–826. [PubMed: 23792628]

Gutierrez-Martinez E, Planes R, Anselmi G, Reynolds M, Menezes S, Adiko AC, Saveanu L, Guermonprez P. Cross-Presentation of Cell-Associated Antigens by MHC Class I in Dendritic Cell Subsets. Front Immunol. 2015; 6:363. [PubMed: 26236315]

Hendel A, Fine EJ, Bao G, Porteus MH. Quantifying on- and off-target genome editing. Trends Biotechnol. 2015; 33:132–140. [PubMed: 25595557]

Hsu PD, Scott DA, Weinstein JA, Ran FA, Konermann S, Agarwala V, Li Y, Fine EJ, Wu X, Shalem O, et al. DNA targeting specificity of RNA-guided Cas9 nucleases. Nat Biotechnol. 2013; 31:827–832. [PubMed: 23873081]

Jackson AL, Bartz SR, Schelter J, Kobayashi SV, Burchard J, Mao M, Li B, Cavet G, Linsley PS. Expression profiling reveals off-target gene regulation by RNAi. Nat Biotechnol. 2003; 21:635–637. [PubMed: 12754523]

Jackson AL, Linsley PS. Noise amidst the silence: off-target effects of siRNAs? Trends Genet. 2004; 20:521–524. [PubMed: 15475108]

Joffre OP, Segura E, Savina A, Amigorena S. Cross-presentation by dendritic cells. Nature reviews Immunology. 2012; 12:557–569.

Kok FO, Shin M, Ni CW, Gupta A, Grosse AS, van Impel A, Kirchmaier BC, Peterson-Maduro J, Kourkoulis G, Male I, et al. Reverse genetic screening reveals poor correlation between morpholino-induced and mutant phenotypes in zebrafish. Dev Cell. 2015; 32:97–108. [PubMed: 25533206]

Koo T, Lee J, Kim JS. Measuring and Reducing Off-Target Activities of Programmable Nucleases Including CRISPR-Cas9. Mol Cells. 2015; 38:475–481. [PubMed: 25985872]

Kool M, Soullié T, van Nimwegen M, Willart MAM, Muskens F, Jung S, Hoogsteden HC, Hammad H, Lambrecht BN. Alum adjuvant boosts adaptive immunity by inducing uric acid and activating inflammatory dendritic cells. The Journal of experimental medicine. 2008; 205:869–882. [PubMed: 18362170]

Li B, Dewey CN. RSEM: accurate transcript quantification from RNA-Seq data with or without a reference genome. BMC Bioinformatics. 2011; 12:323. [PubMed: 21816040]

Love MI, Huber W, Anders S. Moderated estimation of fold change and dispersion for RNA-seq data with DESeq2. Genome Biol. 2014; 15:550. [PubMed: 25516281]

Mantegazza AR, Magalhaes JG, Amigorena S, Marks MS. Presentation of phagocytosed antigens by MHC class I and II. Traffic (Copenhagen, Denmark). 2013; 14:135–152.

Mintern JD, Macri C, Villadangos JA. Modulation of antigen presentation by intracellular trafficking. Current opinion in immunology. 2015; 34C:16–21.

Nair-Gupta P, Baccarini A, Tung N, Seyffer F, Florey O, Huang Y, Banerjee M, Overholtzer M, Roche Paul A, Tampé R, et al. TLR Signals Induce Phagosomal MHC-I Delivery from the Endosomal Recycling Compartment to Allow Cross-Presentation. Cell. 2014; 158:506–521. [PubMed: 25083866]

Nair-Gupta P, Blander JM. An Updated View of the Intracellular Mechanisms Regulating Cross-Presentation. Frontiers in immunology. 2013; 4:401–401. [PubMed: 24319447]

Palmowski MJ, Gileadi U, Salio M, Gallimore A, Millrain M, James E, Addey C, Scott D, Dyson J, Simpson E, et al. Role of immunoproteasomes in cross-presentation. J Immunol. 2006; 177:983–990. [PubMed: 16818754]

Pattanayak V, Lin S, Guilinger JP, Ma E, Doudna JA, Liu DR. High-throughput profiling of off-target DNA cleavage reveals RNA-programmed Cas9 nuclease specificity. Nat Biotechnol. 2013; 31:839–843. [PubMed: 23934178]

Rossi A, Kontarakis Z, Gerri C, Nolte H, Holper S, Kruger M, Stainier DY. Genetic compensation induced by deleterious mutations but not gene knockdowns. Nature. 2015; 524:230–233. [PubMed: 26168398]

Savina A, Jancic C, Hugues S, Guermonprez P, Vargas P, Moura IC, Lennon-Dumenil AM, Seabra MC, Raposo G, Amigorena S. NOX2 controls phagosomal pH to regulate antigen processing during crosspresentation by dendritic cells. Cell. 2006; 126:205–218. [PubMed: 16839887]

Savina A, Peres A, Cebrian I, Carmo N, Moita C, Hacohen N, Moita LF, Amigorena S. The small GTPase Rac2 controls phagosomal alkalinization and antigen crosspresentation selectively in CD8(+) dendritic cells. Immunity. 2009; 30:544–555. [PubMed: 19328020]

Scacheri PC, Rozenblatt-Rosen O, Caplen NJ, Wolfsberg TG, Umayam L, Lee JC, Hughes CM, Shanmugam KS, Bhattacharjee A, Meyerson M, et al. Short interfering RNAs can induce unexpected and divergent changes in the levels of untargeted proteins in mammalian cells. Proc Natl Acad Sci U S A. 2004; 101:1892–1897. [PubMed: 14769924]

Schuette V, Burgdorf S. The ins-and-outs of endosomal antigens for cross-presentation. Current Opinion in Immunology. 2014; 26:63–68. [PubMed: 24556402]

Segura E, Amigorena S. Cross-Presentation in Mouse and Human Dendritic Cells. Adv Immunol. 2015; 127:1–31. [PubMed: 26073982]

Snove O Jr, Holen T. Many commonly used siRNAs risk off-target activity. Biochem Biophys Res Commun. 2004; 319:256–263. [PubMed: 15158470]

Tang BL, Low DY, Hong W. Hsec22c: a homolog of yeast Sec22p and mammalian rsec22a and msec22b/ERS-24. Biochem Biophys Res Commun. 1998; 243:885–891. [PubMed: 9501016]

Zhang T, Wong SH, Tang BL, Xu Y, Hong W. Morphological and functional association of Sec22b/ERS-24 with the pre-Golgi intermediate compartment. Mol Biol Cell. 1999; 10:435–453. [PubMed: 9950687]

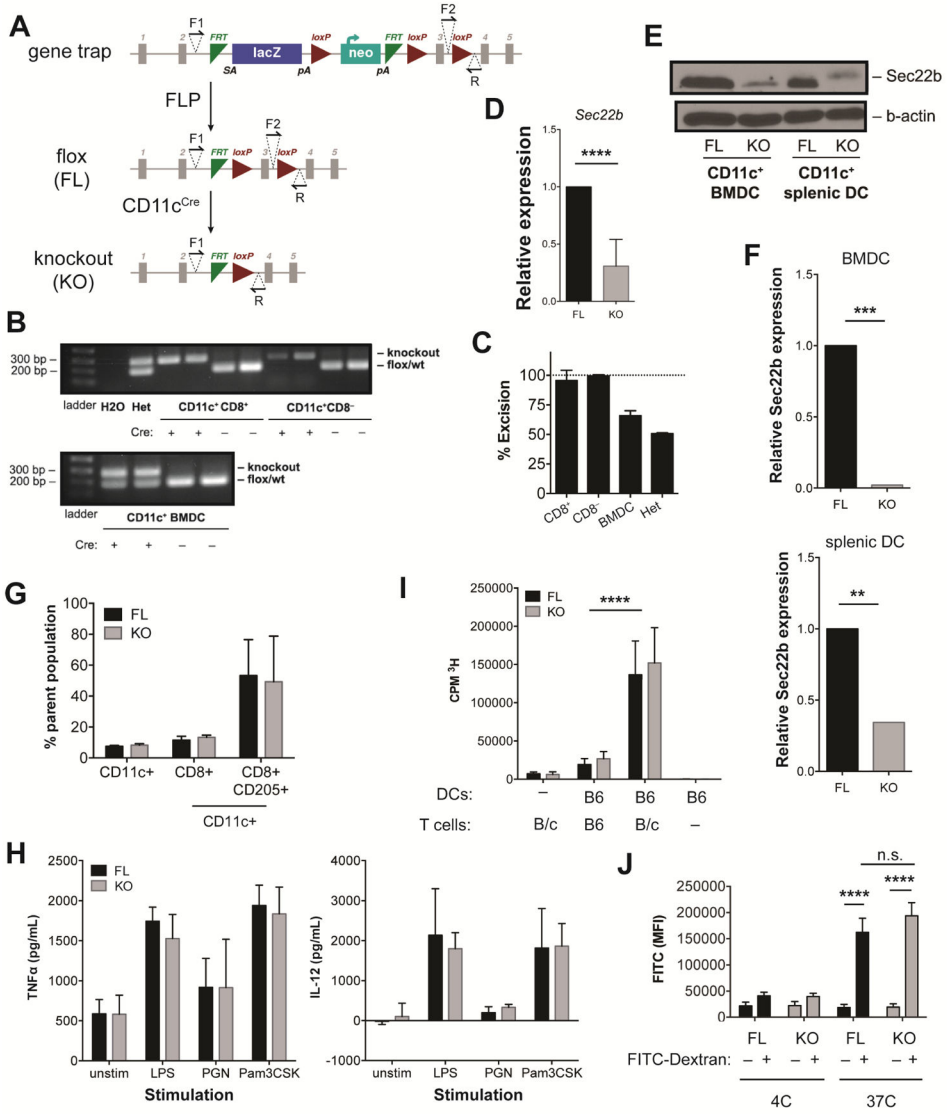

Figure 1. Generation and characterization of a DC-specific SEC22B knockout mouse

(A) DC-specific *Sec22b* knockout (KO) mice were bred from gene-trapped founders using FLP recombinase and *CD11c-Cre* transgenic mice. Half-arrowheads indicate binding sites for forward (F1, F2) and reverse (R) primers used for **(B)** PCR to measure excision of exon 3 in FACS-enriched CD11c^{+} CD8^{+} and CD8^{-} splenic DCs and MACS-enriched CD11c^{+} BMDCs, comparing *CD11c-Cre* (+) to *CD11c-wt* (−) populations. A *Sec22b*$^{+/-}$ mouse was used a heterozygous (het) control for 50% excision. **(C)** Quantification of *Sec22b* exon 3 excision rates in *CD11c-Cre* cell populations. **(D)** qRT-PCR (mean±SEM, n=11) measures *Sec22b* transcript levels in MACS-enriched CD11c^{+} BMDCs and **(E)** Western Blot measures SEC22B protein expression in MACS-enriched CD11c^{+} BMDCs and splenic DCs from *CD11c-Cre Sec22*$^{fl/fl}$ mice (KO) compared to *CD11c-wt Sec22b*$^{fl/fl}$ mice (FL). **(F)** Bar graph quantifies SEC22B protein expression. **(G)** *Ex vivo* flow cytometric immunophenotyping of splenic DC populations plotted as mean proportion of singlets or

indicated parent population±SD (n=3). See related data in Figure S2. **(H)** TNFα and IL-12 production by BMDCs stimulated overnight with TLR ligands lipopolysaccharide (LPS, 500 ng/mL), peptidoglycan (PGN, 5 ug/mL), and Pam3CSK (300 ng/mL) as measured by ELISA and plotted as mean±SEM (n=3). **(I)** Balb/c (B/c) and C57BL/6 (B6) $CD90.2^+$ T cell ^3H-thymidine uptake plotted as mean±SD of triplicate repeats after 4 day stimulation by MACS-sorted $CD11c^+$ splenic DCs from C57BL/6 KO and FL mice, at 40:1 T cell:DC cell ratios. Data is representative of 3 total experiments. **(J)** BMDCs were incubated with FITC-Dextran or 1xPBS vehicle for 30 min at 4C or 37C. Uptake was analyzed by flow cytometry and plotted as mean±SEM (n=4). n.s.= not significant, **$p\leq0.01$, ***$p\leq0.001$, ****$p\leq0.0001$. Purity information on sorted DCs can be found in Figure S1.

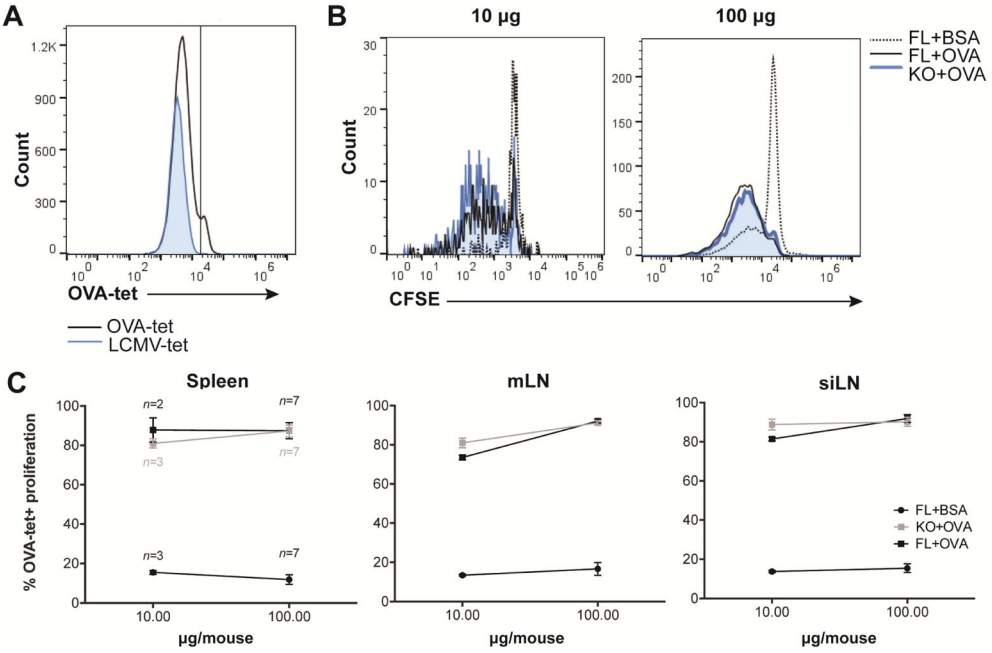

Figure 2. DC-specific SEC22B knockout mice efficiently cross-present antigen *in vivo.*

OVA or BSA was delivered *i.p.* and CFSE-stained OT-I T cells (10^6/mouse) were delivered *i.v.* to FL or KO mice on day 0. On day 7, mice were euthanized and spleen (spl), mesenteric LN (mLN), and superficial inguinal lymph nodes ipsilateral to injection site (siLN) were harvested and flow stained to identify proliferating antigen-specific T cells. **(A)** Representative histogram demonstrating OVA tetramer (OVA-tet; H2-Kb bound to SIINFEKL ($OVA_{257–264}$) peptide) identification of SIINFEKL-restricted $CD3^+$ $CD8^+$ T cells. LCMV tetramer (LCMV-tet; H2-Kb bound to $gp_{34–43}$) used to control for nonspecific binding. **(B)** Representative histograms plotting $CFSE^-$ fraction of OVA-tet^+ cells from spleens of FL or KO mice given either 10 or 100 µg OVA or BSA per mouse. **(C)** Line graphs quantify $CFSE^-$ OVA-tet^+ cells as mean±SD.

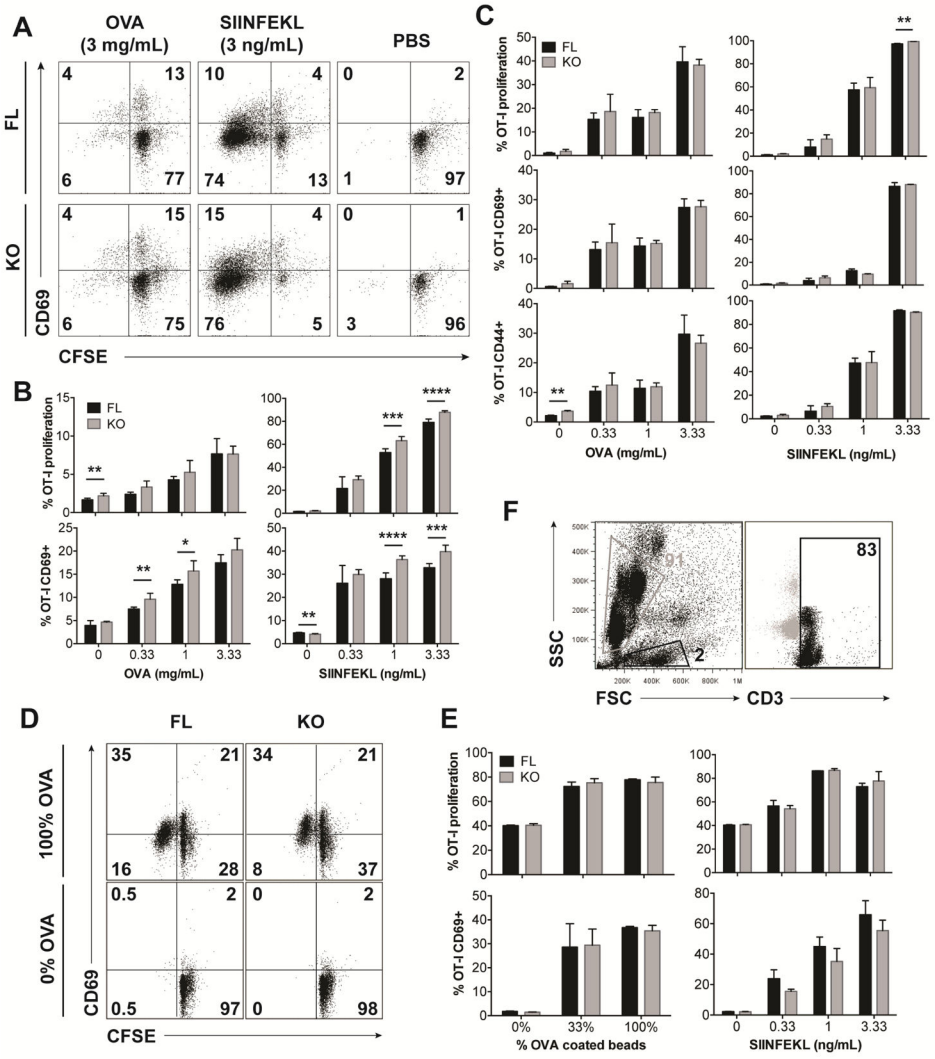

Figure 3. *Sec22b*$^{-/-}$ DCs show no *in vitro* defect in cross-presentation of soluble or particulate antigen

(A, B) CD11c^{+} splenic DCs or **(C)** CD11c^{+} BMDCs loaded with OVA or SIINFEKL peptide were washed, fixed, and cultured with CFSE-stained OT-I T cells. After 3 days, OT-I T cells were harvested and analyzed as shown in the **(A)** representative dot plots. Bar graphs quantify mean±SD **(B, C)** CFSE^{-}, CD69^{+} and **(C)** CD44^{+} populations from triplicate repeats. Panel **(B)** presents data representative of 4 experiments and panel **(C)** presents data representative of 7 experiments. **(D)** CD11c^{+} BMDCs incubated with latex beads coated with varying proportions of OVA to BSA (0% OVA/100% BSA, 33% OVA/66% BSA, or 100% OVA/0% BSA) were washed, fixed, and cultured with CFSE-stained OT-I T cells. After 3 days, OT-I T cells were harvested and analyzed for proliferation and CD69 expression as shown in the representative dot plots. **(E)** Bar graphs quantify mean±SD CFSE^{-} and CD69^{+} populations from triplicate repeats from a representative experiment out of 3. **(F)** Beads were excluded from analysis by size and CD3 expression. *$p \leq 0.05$,

**$p \leq 0.01$, ***$p \leq 0.001$, ****$p \leq 0.0001$. Purity information on sorted DCs can be found in Figure S3. Related experiments can be found in Figures S3 and S4.

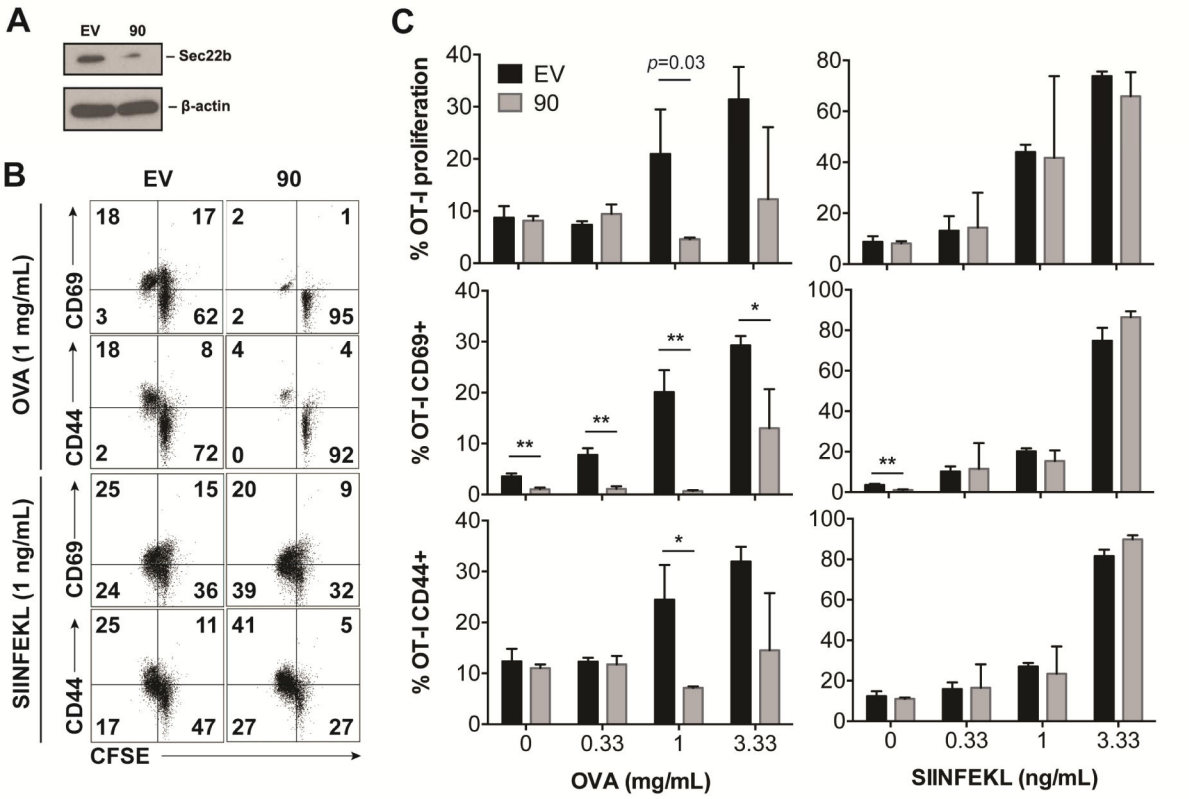

Figure 4. Cross-presentation by BMDCs reduced by *Sec22b* knockdown

(A) Western Blot evaluating reduction in SEC22B expression in C57/BL6 BMDCs after treatment with Sec22b-specific shRNA 90 as compared to empty vector (EV)-treated controls. **(B)** Representative dot plots of CFSE intensity and CD69 and CD44 expression from OT-I T cells after 3 days of co-culture with fixed BMDCs preincubated with OVA or $OVA_{257–264}$ control peptide (SIINFEKL). **(C)** Bar graphs quantify mean±SD of $CFSE^{–}$, $CD69^{+}$, and $CD44^{+}$ populations from triplicate repeats. Data is representative of 3 total experiments. *$p \leq 0.05$, **$p \leq 0.01$.

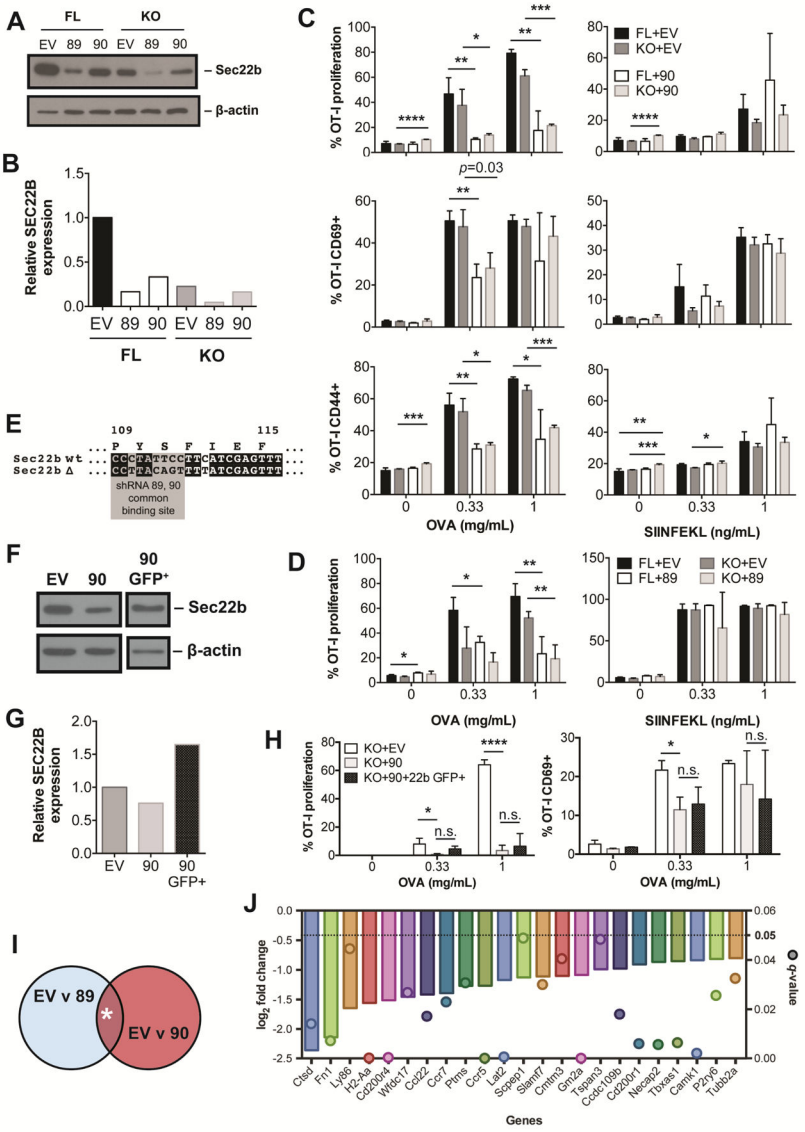

Figure 5. *Sec22b*-targeting shRNA treatment induces cross-presentation defect in KO BMDCs

(A) Western Blot and **(B)** quantification measuring SEC22B expression in FL and KO BMDCs treated with either shRNA 89, 90 or EV. After loading with OVA or SIINFEKL peptide, these BMDCs were washed, fixed, and cultured with CFSE-stained OT-I T cells. After 3 days, T cells were harvested and analyzed for **(C, D)** proliferation and **(C)** expression of CD69 and CD44, quantified in the bar graphs as mean±SD. Panel **(C)** is representative of 3 experiments; panel **(D)** is representative of 2 experiments. Data is plotted as mean±SD of triplicate repeats. **(E)** Sequence alignment of *Sec22b*$^{\Delta}$ transgene to *Sec22b*^{wt} gene, with amino acid sequence indicated above the corresponding codons and the common binding site for shRNA 89 and 90 highlighted in gray. **(F)** Western Blot and **(G)** quantification evaluating SEC22B expression in FACS sorted CD11c^{+} KO BMDCs after treatment with EV control, shRNA 90, or 90 and *Sec22b*$^{\Delta}$ transgene (GFP^{+}). **(H)** KO BMDCs treated with EV, 90, or 90 and *Sec22b*$^{\Delta}$ transgene were incubated with OVA peptide

overnight, washed, fixed, and cultured with CFSE-stained OT-I T cells. After 3 days, T cells were harvested and analyzed for proliferation and CD69 expression. Data is plotted as mean ±SD of triplicate repeats and is representative of 1 experiment **(I)** Ribosomal RNA-depleted RNA from KO BMDCs treated with EV, shRNA 89, or shRNA 90 were sequenced. Highly expressed transcripts, that showed statistically significant downregulation in both shRNA-treatment groups compared to EV groups (*) are **(J)** plotted, with bars representing $\log_2$-fold change compared to EV treatment and dots plotting the associated *q*-values (n=2). n.s. = not significant, *$p \leq 0.05$, **$p \leq 0.01$, ***$p \leq 0.001$, ****$p \leq 0.0001$. Purity information on DC sorting can be found in Figure S1.